

Generating a subwavelength free-space focal spot using a spherical layer

Asaf Farhi

Physics Department and Solid State Institute, Technion, Haifa 32000, Israel

The focal-spot size that is formed by the optical system is one of the main factors in determining the size of objects that can be resolved in imaging. A lens generates a diffraction-limited far-field focal spot which for the optimal case of a uniform illumination, has a full width at half maximum (FWHM) of λ in the lateral axes and 3λ in the axial axis. Here, we utilize resonances in a setup of a spherical layer to generate a far-field subwavelength focal spot at the origin arising from a TM $l = 1$ vector spherical harmonic. To remove the degeneracy associated with the $l = 1$ eigenfunctions of the composite medium, we situate current sources on an axis perpendicular to the spherical layer. The focal spot at the origin is smaller in volume by a factor of up to 27 compared with the one generated by a lens. While there are contributions to the electric field from the other modes in the field expansion and the incoming field, they become negligible close to the resonance. Potential applications are high-resolution three dimensional imaging and precise electromagnetic ablation.

PACS numbers: 42.25.Bs, 42.25.Fx, 42.30.Va

The resolution in microscopy is determined by the size of the focal spot that is generated by the lens. The minimal focal spot, which can be achieved by uniformly illuminating the lens, enables to resolve objects of the size of $\lambda/(2NA)$, where λ is the wavelength and NA is the numerical aperture ($NA \lesssim 1$). This resolution is associated with the lateral axes and in the axial axis objects of the order of 1.5λ can be resolved [5]. For gaussian beams, however, the focal spot is larger and depends on the width of the beam. The optimal lens resolution enables to image most biological cells but not viruses, proteins, and smaller molecules. In a 4π microscope the sample is illuminated from both sides and 5 – 7 times better resolution in the axial axis can be achieved when properly aligning the setup [4]. Techniques based on florescence like STED [8, 11], and PALM and STORM [2, 10] enable subwavelength resolution by stimulating emission at another frequency using an additional torus-like illumination and by enabling to distinguish between the emissions from two kinds of fluorescent molecules, respectively.

It was recently shown that similarly to the situation in phased arrays in which plane currents proportional to a homogeneous medium eigenfunction with a planar geometry generate the same eigenfunction, currents proportional to a vector spherical harmonic (VSH) on a spherical surface generate the same VSH. Interestingly, a TM $l = 1$ VSH near the origin has a far-field focal spot, which is smaller in volume by a factor of ~ 27 compared with the smallest focal spot that can be generated by a lens [7]. It is thus of interest to generate a TM $l = 1$ VSH near the origin to obtain a subdiffraction far-field focal spot. For a medium with a refraction index larger than 1, the TM $l = 1$ field will have even a smaller focal spot. However, the spatial distribution of this VSH is complex and a setup of currents modulated accordingly is experimentally challenging.

We therefore utilize here resonances to naturally generate a TM $l = 1$ VSH. More specifically, our setup is composed of a spherical layer with a permittivity value ϵ_1 which is close to a resonant permittivity value in order

to generate the VSH. Alternatively, a frequency which is close to an eigenfrequency can be used (these eigenvalues can be associated with a gain).

The electromagnetic field expansion for a physical electric field \mathbf{E} can be written as follows [1]

$$\mathbf{E} = \mathbf{E}_0 + \sum_n \frac{s_n}{s - s_n} \frac{\langle \tilde{\mathbf{E}}_n | \mathbf{E}_0 \rangle}{\langle \tilde{\mathbf{E}}_n | \mathbf{E}_n \rangle} |\mathbf{E}_n\rangle, \quad (1)$$

where ϵ_2 is the host-medium permittivity, $s_n \equiv \epsilon_2 / (\epsilon_2 - \epsilon_{1n})$ is the eigenvalue which corresponds to ϵ_{1n} , $s \equiv \epsilon_2 / (\epsilon_2 - \epsilon_1)$, \mathbf{E}_n and $\tilde{\mathbf{E}}_n$ are the eigenfunction and its dual, and \mathbf{E}_0 is the incoming field. $\langle \mathbf{E}_1 | \mathbf{E}_2 \rangle = \int d\mathbf{r} \theta_1(\mathbf{r}) \mathbf{E}_1 \cdot \mathbf{E}_2$ and $\theta_1(\mathbf{r})$ is a window function which equals 1 inside the inclusion volume. Thus, when ϵ_1 is close to ϵ_{1n} , the corresponding VSH has a large contribution in the electric field expansion. Clearly, other modes and the incoming field exist in the expansion. Fortunately, close to a resonance the TM $l = 1$ eigenfunction will have the dominant contribution.

Still, VSHs have a degeneracy in the m index, which usually results in the generation of all the m modes as a response to an incoming electric field. We therefore employ the current formulation of the field expansion in order to remove this degeneracy. In this formulation we express the incoming field in terms of Green's tensor $\mathbf{E}_0(\mathbf{r}) = \int dV \overleftrightarrow{G}(\mathbf{r}', \mathbf{r}) \cdot \mathbf{J}(\mathbf{r})$ and substitute it in $\langle \tilde{\mathbf{E}}_n | \mathbf{E}_0 \rangle$. Then we change the order of integration and use the definition of the eigenfunction to obtain [6]

$$\begin{aligned} \langle \tilde{\mathbf{E}}_n | \mathbf{E}_0 \rangle &= -\frac{4\pi i}{\epsilon_2 \omega} \int dV' \theta_1(\mathbf{r}') \mathbf{E}_n(\mathbf{r}') \cdot \int dV \overleftrightarrow{G}(\mathbf{r}', \mathbf{r}) \cdot \mathbf{J} \\ &= -\frac{4\pi i}{\epsilon_2 \omega} s_n \int dV \mathbf{E}_n(\mathbf{r}) \cdot \mathbf{J}_{\text{dip}}(\mathbf{r}) = -\frac{4\pi s_n}{\epsilon_2} \mathbf{p} \cdot \mathbf{E}_n(\mathbf{r}_0), \end{aligned}$$

where $\mathbf{J}_{\text{dip}}(\mathbf{r})$ is an oscillating point electric dipole, \mathbf{p} is the dipole moment, and ω is the oscillation frequency.

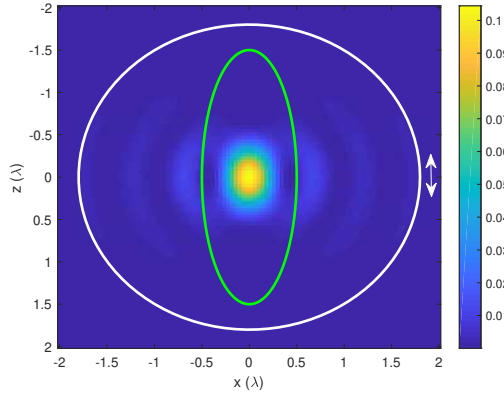


Figure 1: A setup composed of a spherical layer (white) and an oscillating dipole, and the intensity of the generated focal spot arising from a TM $l = 1$ eigenmode. The external ellipse is the optimal focal spot that can be achieved by a lens (green, corresponds to the green in the spherical-layer focal spot). The size of the spherical layer and the location of the oscillating dipole can vary.

Now the expansion of the electric field reads

$$\mathbf{E} = \mathbf{E}_0 - \frac{4\pi}{\epsilon_2} \sum_n \frac{s_n^2}{s - s_n} \frac{\mathbf{p} \cdot \tilde{\mathbf{E}}_n(\mathbf{r}_0)}{\langle \tilde{\mathbf{E}}_n | \mathbf{E}_n \rangle} |\mathbf{E}_n\rangle. \quad (2)$$

Thus, situating an oscillating dipole or cylinder perpendicular to the spherical layer will result in the generation of a TM $l = 1$ mode (see Fig. 1).

The general form of a TM VSH is [9]

$$\mathbf{E}_l^{(E)} \propto \frac{1}{\epsilon(r)} \nabla \times f_l(kr) \mathbf{X}_{lm}, \quad \mathbf{X}_{lm} = \frac{1}{\sqrt{l(l+1)}} \mathbf{L} Y_{lm},$$

$$f_l(kr) = A_l^{(1)} h_l^{(1)}(kr) + A_l^{(2)} h_l^{(2)}(kr),$$

where $f_l(r)$ is a linear combination of spherical Hankel functions, $h_l(r)$ is a spherical Hankel function, k is the wavevector, and $\mathbf{L} = \frac{1}{i}(\mathbf{r} \times \nabla)$.

For a spherical layer in $r_1 < r < r_2$, $f_l(r)$ that satisfies boundary conditions is of the form

$$f_l(r) = \begin{cases} C_l h_l^{(1)}(k_2 r) & r > r_2 \\ B_l^{(1)} h_l^{(1)}(k_{1n} r) + B_l^{(2)} h_l^{(2)}(k_{1n} r) & r_1 < r < r_2 \\ A_l j_l(k_2 r) & r < r_1 \end{cases},$$

where $j_l(r)$ is a spherical Bessel function and k_{1n}, k_2 correspond to $\epsilon_{1n}, \epsilon_2$, respectively.

From continuity of tangential \mathbf{E} and \mathbf{H} we have for a TM eigenfunction

$$f_l(r_1^-) = f_l(r_1^+), \quad f_l(r_2^-) = f_l(r_2^+),$$

$$\frac{\partial(r f_l(r))}{\partial r} \Big|_{r=r_1^-} = \frac{1}{\epsilon_{1n}} \frac{\partial(r f_l(r))}{\partial r} \Big|_{r=r_1^+},$$

$$\frac{1}{\epsilon_{1n}} \frac{\partial(r f_l(r))}{\partial r} \Big|_{r=r_2^-} = \frac{\partial(r f_l(r))}{\partial r} \Big|_{r=r_2^+}.$$

Similarly for a TE eigenfunction we write

$$\mathbf{E}_l^{(M)} \propto f_l(kr) \mathbf{X}_{lm},$$

with the boundary conditions

$$f_l(r_1^-) = f_l(r_1^+), \quad f_l(r_2^-) = f_l(r_2^+),$$

$$\frac{\partial(r f_l(r))}{\partial r} \Big|_{r=r_1^-} = \frac{\partial(r f_l(r))}{\partial r} \Big|_{r=r_1^+},$$

$$\frac{\partial(r f_l(r))}{\partial r} \Big|_{r=r_2^-} = \frac{\partial(r f_l(r))}{\partial r} \Big|_{r=r_2^+}.$$

The eigenfunctions in the radiation zone can be expressed as [9]

$$\mathbf{E} \rightarrow Z_0 \mathbf{H} \times \mathbf{n},$$

where $\mathbf{n} = \mathbf{r}/r$. Hence, since \mathbf{H}_{TM} is parallel to the sphere surface \mathbf{E}_{TM} is also parallel to the sphere surface. Thus, due to the inner product in Eq. (2), when an oscillating dipole is placed in the radiation zone it may excite a mode if it is oriented parallel to the spherical layer surface.

For concreteness, we situate an oscillating dipole outside the spherical layer on the positive x axis. The z components of the TE eigenfunctions can be found from [9]

$$E_{l,mz}^{\text{TE}} = (\mathbf{L} Y_{lm})_z = m Y_{lm}.$$

The z components of the TM eigenfunctions readily follow from the two relations above. The z components of the $l = 1$ modes on the positive x axis in the radiation zone are

$$E_{l=1,m=0z}^{\text{TM}} \neq 0, \quad E_{l=1,m=\pm 1z}^{\text{TM}} = 0,$$

$$E_{l=1,m=0z}^{\text{TE}} = 0, \quad E_{l=1,m=\pm 1z}^{\text{TE}} \neq 0.$$

Thus, by placing an oscillating dipole on the x axis directed along the z axis we have removed the m degeneracy of the TM modes. In addition, to have a dominant

contribution of this mode, the physical permittivity has to be much closer to the corresponding eigenpermittivity compared with its distances from the eigenpermittivities of the other modes. The high order modes have a minor contribution to the expansion and we can focus on a certain l range when comparing these distances [3].

The resonant permittivity usually has an imaginary part that corresponds to gain. While incorporating gain in the spherical layer will bring the system to a resonance, if a real valued permittivity will be close enough to a resonance, a similar effect is expected. The spacing between resonances and the imaginary part of the permittivity depend on the thickness of the spherical layer. A thin spherical layer will result in a large eigenpermittivity gain and largely spaced resonances. A thick spherical layer will result in a small imaginary part of the eigenpermittivity and more closely spaced resonances. Thus, in order to balance between these effects for a real valued permittivity, a spherical layer thickness at an intermediate region of $\sim \lambda/4$ may be desirable.

An additional degeneracy arises when $r_1, r_2 \gtrsim 10\lambda$ since at the $r \gg \lambda$ limit $j_l, h_l^{(1)}$ have the form

$$j_l(r) \rightarrow \frac{1}{r} \sin\left(r - \frac{l\pi}{2}\right), \quad h_l^{(1)}(r) \rightarrow (-i)^{l+1} \frac{e^{ir}}{r}.$$

As a result the even and odd eigenvalues can be very similar. A possible way to remove this degeneracy is to slightly change the structure so that the eigenfunctions and the eigenvalues will change. For example the spheri-

cal layer can be capped from above (or in several places), which will also enable to easily place objects inside. Alternatively, two half spherical layers with different sizes may be used.

We introduced a setup of a spherical layer, that close to a resonance can achieve a subwavelength far-field focal spot. The degeneracy of the excited mode is removed by incorporating currents on an axis which is perpendicular to the spherical layer. Such currents can be realized by a medium polarized due to an impinging electric field. Interestingly, The field emitted by the polarized medium at the focal spot excites the spherical layer mode, which reexcites the medium at the focal spot etc. This coupling can enhance the emission from the medium at the focal spot. Also, near a resonance the field can become very strong and may enable larger penetration of ballistic photons and enhancement of the signal generated at the focal spot by the spherical layer. To image from the focal spot, one can think of collecting light from the other side of the spherical layer by means of a lens or another optical element. This signal is mostly composed of the sum of the excitation of the TM $l = 1$ mode due to the sources and the polarized medium at the focal spot. To further minimize the effective focal spot size nonlinear optics or techniques such as PALM or STORM [2, 10] can be used. In addition, the TM $l = 2$ and TE $l = 1$ modes have a torus shape [7] and may be used to stimulate fluorescence emission at another wavelength similar to STED [8, 11]. Potential applications are high-resolution 3D imaging and precise tissue ablation.

[1] David J Bergman and D Stroud. Theory of resonances in the electromagnetic scattering by macroscopic bodies. *Physical Review B*, 22(8):3527, 1980.

[2] Eric Betzig, George H Patterson, Rachid Sougrat, O Wolf Lindwasser, Scott Olenych, Juan S Bonifacino, Michael W Davidson, Jennifer Lippincott-Schwartz, and Harald F Hess. Imaging intracellular fluorescent proteins at nanometer resolution. *Science*, 313(5793):1642–1645, 2006.

[3] Craig F Bohren and Donald R Huffman. *Absorption and scattering of light by small particles*. John Wiley & Sons, 2008.

[4] Christoph Cremer and Thomas Cremer. Considerations on a laser-scanning-microscope with high resolution and depth of field. *Microscopica acta*, pages 31–44, 1974.

[5] Christoph Cremer and Barry R Masters. Resolution enhancement techniques in microscopy. *The European Physical Journal H*, 38(3):281–344, 2013.

[6] Asaf Farhi and David J Bergman. Electromagnetic eigenstates and the field of an oscillating point electric dipole in a flat-slab composite structure. *Physical Review A*, 93(6):063844, 2016.

[7] Asaf Farhi and David J Bergman. Generating an electromagnetic multipole by oscillating currents. *Physical Review A*, 96(2):023857, 2017.

[8] Stefan W Hell and Jan Wichmann. Breaking the diffraction resolution limit by stimulated emission: stimulated-emission-depletion fluorescence microscopy. *Optics letters*, 19(11):780–782, 1994.

[9] John David Jackson. *Classical electrodynamics*. John Wiley & Sons, 2012.

[10] William E Moerner and Lothar Kador. Optical detection and spectroscopy of single molecules in a solid. *Physical review letters*, 62(21):2535, 1989.

[11] VA Okhonin. Method of investigating specimen microstructure. *Patent SU*, 1374992, 1986.